0026-895X/02/6104-768–777$7.00
MOLECULAR PHARMACOLOGY
Copyright © 2002 The American Society for Pharmacology and Experimental Therapeutics
Mol Pharmacol 61:768–777, 2002

Vol. 61, No. 4
1398/974599
Printed in U.S.A.

Side-Chain Substitutions within Angiotensin II Reveal Different Requirements for Signaling, Internalization, and Phosphorylation of Type 1A Angiotensin Receptors

ALICE C. HOLLOWAY, HONGWEI QIAN, LUISA PIPOLO, JAMES ZIOGAS, SHIN-ICHIRO MIURA, SADASHIVA KARNIK, BRIDGET R. SOUTHWELL, MICHAEL J. LEW, and WALTER G. THOMAS

Molecular Endocrinology Laboratory, Baker Medical Research Institute, Melbourne, Australia (A.C.H., H.Q., L.P., W.G.T.); Department of Pharmacology, University of Melbourne, Parkville, Australia (J.Z., M.J.L.); Department of Molecular Cardiology, Cleveland Clinic Foundation, Cleveland, Ohio (S.-I.M., S.K.); and Department of Gastrology and Nutrition, Murdoch Childrens Research Institute, Royal Children's Hospital, Parkville, Australia (B.R.S.)

Received October 1, 2001; accepted January 14, 2002

This article is available online at http://molpharm.aspetjournals.org

ABSTRACT

Binding of the peptide hormone angiotensin II (AngII) to the type 1 (AT_{1A}) receptor and the subsequent activation of phospholipase C-mediated signaling, involves specific determinants within the AngII peptide sequence. In contrast, the contribution of such determinants to AT_{1A} receptor internalization, phosphorylation and activation of mitogen-activated protein kinase (MAPK) signaling is not known. In this study, the internalization of an enhanced green fluorescent protein-tagged AT_{1A} receptor (AT_{1A}-EGFP), in response to AngII and a series of substituted analogs, was visualized and quantified using confocal microscopy. AngII-stimulation resulted in a rapid, concentration-dependent internalization of the chimeric receptor, which was prevented by pretreatment with the nonpeptide AT_1 receptor antagonist EXP3174. Remarkably, AT_{1A} receptor internalization was unaffected by substitution of AngII side chains, including single and double substitutions of Tyr^4 and Phe^8 that abolish phospholipase C signaling through the receptor. AngII-induced receptor phosphorylation was significantly inhibited by several substitutions at Phe^8 as well as alanine replacement of Asp^1. The activation of MAPK was only significantly inhibited by substitutions at position eight in the peptide and specific substitutions did not equally inhibit inositol phosphate production, receptor phosphorylation and MAPK activation. These results indicate that separate, yet overlapping, contacts made between the AngII peptide and the AT_{1A} receptor select/induce distinct receptor conformations that preferentially affect particular receptor outcomes. The requirements for AT_{1A} receptor internalization seem to be less stringent than receptor activation and signaling, suggesting an inherent bias toward receptor deactivation.

The peptide hormone angiotensin II (AngII; Asp^1-Arg^2-Val^3-Tyr^4-Ile/Val^5-His^6-Pro^7-Phe^8), activates type 1 angiotensin receptors (AT_1) to maintain arterial blood pressure and cardiovascular homeostasis. AT_1 receptors (AT_{1A} and AT_{1B} in rodents) are seven transmembrane-spanning receptors that couple to $G_{\alpha q/11}$-phospholipase C-β1, leading to intracellular inositol trisphosphate (IP_3) production, calcium mobilization, and activation of protein kinase C. In addition, activated AT_1 receptors couple to mitogen-activated protein kinase (MAPK) and receptor- and soluble-tyrosine kinase pathways (de Gasparo et al., 2000). The high-affinity binding (K_D, ~1 nM) of AngII to the AT_1 receptor, and its subsequent activation, results from multiple interactions between discrete amino acid side chains in AngII and specific residues on the receptor positioned by the arrangement of the seven transmembrane domains. Specifically, two key pairings, Arg^2 (AngII) with Asp^{281} (receptor) and the α-carboxyl of Phe^8 (AngII) with Lys^{199} (receptor), convey high-affinity binding but seem less important for receptor coupling to IP_3 generation (Feng et al., 1995; Noda et al., 1995). This initial docking positions the aromatic side chains of Tyr^4 and Phe^8 (AngII) to engage, respectively, Asn^{111} and His^{256} on the receptor, which instigates receptor activation, coupling to G protein(s) and subsequent phospholipase C-mediated signals (Noda et al., 1995; Noda et al., 1996), but contributes a smaller amount to binding affinity.

The ligand-mediated activation of AT_1 receptors is accompanied by ancillary regulatory events, including receptor

This work was supported by a National Health and Medical Research Council of Australia Institute Block Grant to the Baker Medical Research Institute, National Heart Foundation of Australia grant-in-aid G99M0301 (to W.G.T), and National Institutes of Health grant HL57470 (to S.K.).

ABBREVIATIONS: AngII, angiotensin II; AT_{1A}, type I angiotensin receptor; IP_3, inositol trisphosphate; MAPK, mitogen activated protein kinase; GPCR, G protein-coupled receptor; NHA, N-terminal hemagglutinin epitope tag; EGFP, enhanced green fluorescent protein; CHO-K1, Chinese hamster ovary cells; ARBB, angiotensin receptor binding buffer; WGA-TR, wheat germ agglutinin-Texas Red; HBSS, Hank's buffered salt solution; PAGE, polyacrylamide gel electrophoresis; HA, hemagglutinin.

phosphorylation, arrestin binding and receptor internalization (Thomas, 1999; Hunyady et al., 2000; Oakley et al., 2001). These processes are initiated soon after ligand-receptor interaction and may contribute to rapid receptor desensitization. The AT_1 receptor is phosphorylated by both G protein-coupled receptor (GPCR) kinases and protein kinase C on specific carboxyl-terminal serine and threonine residues (Thomas, 1999; Hunyady et al., 2000). Phosphorylation by GPCR kinases presumably produces a high-affinity binding site for arrestins, which sterically hinder further G protein coupling and act as adapters for the cellular internalization machinery (Lefkowitz, 1998). Alternatively, arrestins may act as scaffolds to recruit additional signaling molecules, including tyrosine kinases and MAPKs, to GPCRs (Pierce et al., 2001). Phosphorylation of the AT_{1A} receptor carboxyl terminus has been implicated in rapid agonist-induced endocytosis (Smith et al., 1998; Thomas et al., 1998), presumably via arrestin recruitment (Oakley et al., 2001).

Recent evidence indicates that multiple conformations exist for the AT_{1A} receptor, some coupling the receptor to signaling pathways and others directing receptor phosphorylation or internalization (Thomas et al., 2000). The transition of the AT_{1A} receptor through these various states may be induced or stabilized by specific AngII side chains during the docking of ligand onto receptor, because separate residues within the AngII peptide confer high-affinity binding and IP_3 signaling capacity (Feng et al., 1995; Noda et al., 1995; Noda et al., 1996). The phenomenon of ligand-specific receptor states has been referred to as agonist-receptor trafficking (Kenakin, 1995) or biased agonism (Jarpe et al., 1998). This raises a question: do specific points of contact between AngII and the AT_{1A} receptor induce/stabilize discrete receptor states that dictate receptor processes, such as internalization, phosphorylation, and MAPK activation?

In this study, we examined the capacity of AngII and a series of substituted analogs to promote phosphorylation and internalization of the AT_{1A} receptor and MAPK signaling. We observed a key role for Phe^8 of AngII in receptor phosphorylation and activation of MAPK, with important differences in tolerance to specific substitutions. In contrast, receptor internalization, as visualized by confocal microscopy of an enhanced green fluorescent protein-tagged AT_{1A} receptor, was unaffected by substitutions at any position in AngII.

Materials and Methods

AngII Analogs. For AngII analogs used in this study, see Table 1.

The AT_{1A}-Enhanced Green Fluorescent Protein Receptor. An N-terminal hemagglutinin epitope-tagged AT_{1A} receptor (NHA-AT_{1A}) (Thomas et al., 1998) was amplified using polymerase chain reaction with T_7 primer (sense), upstream of a unique *Hin*dIII site, and an antisense primer (5′-CAGGATCCCCCTCCACCTCAAAACAAGACGCAGG-3′), which removed the stop codon from the receptor and incorporated a *Bam*HI site (underlined). The polymerase chain reaction product was digested with *Hin*dIII and *Bam*HI and inserted into the multiple cloning site of the pEGFP-N1 vector to generate an NHA-AT_{1A}-EGFP fusion construct. The construct was sequenced to confirm the integrity of the AT_{1A} coding region and the fusion to EGFP.

Cell Culture and Transfection. Chinese hamster ovary (CHO-K1) cells were maintained in α-minimum essential medium containing 10% fetal bovine serum supplemented with antibiotics and antimycotics (complete media). Cells were transferred to 12-well plastic culture dishes, grown to 70% confluence, and transiently transfected using LipofectAMINE as described previously (Thomas et al., 1998), with 0.025 μg of NHA-AT_{1A} or NHA-AT_{1A}-EGFP receptor plasmid DNA and 0.6 μg of vector plasmid DNA per well. For eight-well slides, cells were seeded at a density of 100,000 to 140,000 cells/well, grown overnight, and transfected with LipofectAMINE (1.4 μl/well), NHA-AT_{1A}-EGFP receptor plasmid DNA (7 ng/well), and vector DNA (164 ng/well). All transfected cells were grown in complete media for 48 h and serum-starved overnight before experiments.

Radioligand Binding Assays. Radioligand binding assays on transiently transfected CHO-K1 cells were performed as described previously (Thomas et al., 1995) using the AngII antagonist [^{125}I]Sar^1Ile^8AngII as tracer. Equilibrium binding was for 5 h at 4°C.

Radioligand Internalization Assay. CHO-K1 cells expressing the NHA-AT_{1A} or NHA-AT_{1A}-EGFP receptor were incubated for 1, 2, 5, 10, or 20 min at 37°C with [^{125}I]AngII. They were then washed; cell

TABLE 1
Angiotensin II analogs used in this study
Maximum IP production is reported as a percentage of [Sar^1]-AngII.

Peptide	1	2	3	4	5	6	7	8	Code	K_D (AT1R)	Max IP Production
										nM	%
AngII	**NH_2-Asp-**	**Arg-**	**Val-**	**Tyr-**	**Val-**	**His-**	**Pro-**	**Phe-COOH**		1.6[a]	100
[Sar^1Ala^4]AngII	Sar-	Arg-	Val-	**Ala-**	Val-	His-	Pro-	Phe-COOH	(A4)	150[a]	90[a]
[Sar^1Ala^8]AngII	Sar-	Arg-	Val-	Tyr-	Val-	His-	Pro-	**Ala-**COOH	(A8)	0.9[a]	18[a]
[$Sar^1Ile^4Ile^8$]AngII	Sar-	Arg-	Val-	**Ile-**	Val-	His-	Pro-	**Ile-**COOH	(I48)	300[a]	0[a]
[$Sar^1Gly^4Gly^8$]AngII	Sar-	Arg-	Val-	**Gly**	Val-	His-	Pro-	**Gly-**COOH	(G48)	310[c]	0[c]
AngIII	NH_2-	Arg-	Val-	Tyr-	Val-	His-	Pro-	Phe-COOH		8.9[c]	86[c]
[Ala^1]AngII	NH_2-**Ala-**	Arg-	Val-	Tyr-	Val-	His-	Pro-	Phe-COOH	(A1)	0.9[a]	100[a]
[Sar^1Gln^2]AngII	Sar-	**Gln-**	Val-	Tyr-	Val-	His-	Pro-	Phe-COOH	(G2)	8.1[a]	92[a]
[Sar^1Ala^3]AngII	Sar-	Arg-	**Ala-**	Tyr-	Val-	His-	Pro-	Phe-COOH	(A3)	18[a]	95[a]
[Sar^1Ala^6]AngII	Sar-	Arg-	Val-	Tyr-	Val-	**Ala-**	Pro-	Phe-COOH	(A6)	103[a]	92[a]
[Sar^1Ala^7]AngII	Sar-	Arg-	Val-	Tyr-	Val-	His-	**Ala-**	Phe-COOH	(A7)	91[a]	98[a]
[Sar^1]AngII-amide	Sar-	Arg-	Val-	Tyr-	Val-	His-	Pro-	Phe-**$CONH_2$**	(Am)	7.3[a]	85[b]
[Sar^1Cha^4]AngII	Sar-	Arg-	Val-	**Cha-**	Val-	His-	Pro-	Phe-COOH	(C4)	75.9[a]	48[a]
[Sar^1Cha^8]AngII	Sar-	Arg-	Val-	Tyr-	Val-	His-	Pro-	**Cha-**COOH	(C8)	0.47[a]	40[a]
[Sar^1Ile^8]AngII	Sar-	Arg-	Val-	Tyr-	Val-	His-	Pro-	**Ile-**COOH	(I8)	0.37[a]	20[a]
[Sar^1DiP^8]AngII	Sar-	Arg-	Val-	Tyr-	Val-	His-	Pro-	**DiP-**COOH	(D8)	0.89[c]	100[c]

Sar, sarcosine, *N*-methyl glycine; Cha, β-cyclohexylalanine; Dip, diphenylalanine
[a] Miura and Karnik (1999).
[b] Noda et al. (1995).
[c] S. Miura and S. S. Karnik, unpublished observations.

surface-bound ligand was stripped by acid-washing and collected. Radioactivity associated with the cells (internalized) was determined as a percentage of the total (acid wash plus cell-associated) (Thomas et al., 1998).

Cytosensor Microphysiometer Signaling Assay. CHO-K1 cells transiently transfected with NHA-AT_{1A} or NHA-AT_{1A}-EGFP were plated into 12-mm Transwells (3-μm pore diameter) at a density of 250,000 cells/well and grown overnight. Transwells with spacers and capsule inserts were placed in the sensor chambers and the cells were allowed to equilibrate for 1 to 2 h. When a steady state was achieved, AngII accumulative concentration-response curves were constructed over the concentration range 10^{-11} to 10^{-6} M. Responses were measured as the rate of change of pH, both as a voltage change and as a percentage change from baseline voltage (normalized to 100%) using Cytosoft software.

Receptor Internalization Measured by Confocal Microscopy. CHO-K1 cells were seeded in eight-well chamber slides at a density of 100,000 cell/well, transfected as described above, incubated in complete media for 36 h, and serum-deprived overnight. Cells were equilibrated (37°C, 1 h) in 0.4 ml of angiotensin receptor binding buffer (ARBB): 50 mM Tris-HCl, pH 7.4, containing 120 mM NaCl, 4 mM KCl, 5 mM $MgCl_2$, 1 mM $CaCl_2$, 10 μg/ml bacitracin, 2 mg/ml D-glucose, and 0.25% bovine serum albumin. Ligands were added to give a final concentration of 100 times their respective published K_D values (see Table 1) and slides were incubated at 37°C for 20 min. For AngII concentration-response experiments, cells were stimulated with 0, 10^{-11}, 10^{-10}, 10^{-9}, 10^{-8}, and 10^{-7} M AngII. Wells were aspirated and cells fixed with 4% paraformaldehyde in sodium phosphate buffer, pH 7.4 (0.5 ml), for 20 min at room temperature, washed with ARBB, incubated in ARBB with 10% fetal bovine serum and 100 mM glycine for 10 min, washed, and incubated with wheat-germ agglutinin/Texas Red (WGA-TR) conjugate (2 μg/ml) for 30 min at room temperature. WGA-TR was crosslinked to cells by incubating in 4% paraformaldehyde for 20 min. Chambers were removed from the slide, washed twice with Hanks' buffered salt solution (HBSS) and mounted in 90% glycerol/10% HBSS. All stimulations were performed coded and protocols withheld until after analysis of confocal imaging.

Slides were examined on an MRC1024-Zeiss Axioplan 2 confocal microscope with krypton/argon laser (Bio-Rad, Hercules, CA). All sections were scanned with a Plan Apochromat 63×, 1.40 numerical aperture, oil-immersion objective and 3× digital zoom (box size, 58.8 × 58.8 μm). Green and red channel images were collected simultaneously using excitation at 488 nm for EGFP and 568 nm for Texas Red and laser intensity was kept constant for each experiment (10% or 30% power). Optical sections were taken through cells (nine cells/treatment) expressing a medium level of the NHA-AT_{1A}-EGFP receptor. For each cell, a single optical section was collected at a point where the nucleus was largest and there was a clear outline of the plasma membrane. Images were collected by LaserSharp acquisition software and quantified as described previously (Southwell et al., 1998).

Location of AT_{1A} receptors on the surface or in the cytoplasm was quantified (Optimas ver. 6.0) by comparing the fluorescence of EGFP (receptor) with that of WGA-TR (labels the cell surface). Although WGA-TR was visible as red fluorescence on the cell surface only, EGFP was visible in the green channel and was located on the cell surface and in the cytoplasm. Intracellular EGFP fluorescence was calculated by subtracting cell surface EGFP fluorescence, which colocalized with WGA-TR, from total EGFP fluorescence.

MAPK Activation. Serum-starved CHO-K1 cells expressing the AT_{1A} receptor (in 12 well plates) were stimulated for 4 min with AngII or the substituted AngII analogs (Table 1), rapidly washed twice with ice-cold HBSS, and lysed in 250 μl of radioimmunoprecipitation buffer (50 mM Tris, pH 7.4, 100 mM NaCl, 2 mM EDTA, 50 mM sodium fluoride, 10 mM sodium pyrophosphate, 1% Triton X-100, 0.5% sodium deoxycholate, 0.1% SDS, 1 μg/ml aprotinin, 5 μg/ml leupeptin, and 1 μg/ml pepstatin) for 30 min at 4°C. Cell lysates were centrifuged at 14,000*g* for 15 min and 10 μl of supernatant was resolved on SDS-PAGE and Western blotted. Western blots were probed with a monoclonal antibody (E10) to phospho-p44/42 MAPK (T202/Y204) to identify the phosphorylated (active) forms of MAPK and developed by enhanced chemiluminescence. Blots were subsequently reprobed with a rabbit polyclonal antibody (SC93) to detect total MAPK. Blots were quantified using Scion Image software.

Receptor Phosphorylation Assay. The procedure for receptor phosphorylation has been described previously (Thomas et al., 1998). ^{32}P-loaded cells were stimulated (10 min, 37°C) with AngII and the various substituted analogs at a concentration 100 times that of the K_D for the receptor. HA-tagged AT_{1A} receptors were immunoprecipitated using anti-HA antibody (12CA5) and phosphorylated receptor resolved by 10% SDS-PAGE and a filmless autoradiographic system (Fujix Bio-imaging Analyzer BAS 1000; Fuji, Tokyo, Japan).

Equipment and Reagents. Equipment and reagents used and their source are as follows: CHO-K1 cells (American Type Culture Collection, Manassas, VA); cell culture media, additives, LipofectAMINE, pEGFP-N1 vector (Invitrogen, Melbourne, Australia); cell culture dishes and 12-mm transwells (Costar, Acton, MA); eight-well glass chamber slides (Nalge Nunc International, Naperville, IL); [^{32}P]orthophosphate (ICN Biomedicals, Costa Mesa, CA); protein A-agarose (Roche Applied Science, Melbourne, Australia); wheat germ agglutinin/Texas Red conjugate (Molecular Probes, Eugene, OR); angiotensin II (Auspep, Melbourne, Australia); [^{125}I]AngII and [^{125}I]Sar^{1}Ile^{8}AngII (specific activity, ~2000 Ci/mmol; Austin Biomedical Services, Melbourne, Australia); other AngII analogs were synthesized in the Cleveland Clinic Core synthesis facility (Cleveland, OH). The MAPK antibodies E10 and SC93 were from Cell Signaling Technologies (Beverly, MA) and Santa Cruz Biotechnology (Santa Cruz, CA), respectively. All other chemicals were bought from Sigma (Sydney, Australia) or BDH (Kilsyth, Melbourne, Australia); Cytosensor Microphysiometer and Cytosoft software (Molecular Devices, Menlo Park, CA); LaserSharp Acquisition software (Bio-Rad, Hercules, CA); Optimas Image Analysis (Media Cybernetics, Del Mar, CA) and Scion Image software (Scion, Frederick, MD).

Statistical Analysis. Statistics performed were the unpaired *t* test and one-way analysis of variance (Newman-Keuls multiple-comparison test) calculated by Prism data analysis software (v.2.0; GraphPad, San Diego, CA). Figures are presented as mean ± S.E.

Results

Comparison of the AT_{1A}-EGFP and Wild-Type Receptors. To examine the internalization of AT_{1A} receptors, we generated a NHA-AT_{1A}-EGFP chimera suitable for following receptor trafficking by confocal microscopy. Figure 1 shows a comparison of receptor binding, signaling and internalization for the wild-type (NHA-AT_{1A}) and NHA-AT_{1A}-EGFP receptors. Competition binding studies, using the radio-labeled peptide antagonist [^{125}I]Sar^{1}Ile^{8}AngII, demonstrated that both receptors expressed equally well in CHO-K1 cells (~1000 fmol of receptor/mg of protein) and displacement experiments with AngII, EXP3174 (an AT_1-selective nonpeptide antagonist), or PD123319 (an AT_2-selective nonpeptide antagonist) yielded identical binding profiles (Fig. 1A). AngII displaced the iodinated ligand with pK_I values of 8.13 ± 0.06 for the NHA-AT_{1A} receptor and 8.10 ± 0.08 for the NHA-AT_{1A}-EGFP receptor. pK_I values for the AT_1 receptor selective nonpeptide antagonist, EXP3174, were calculated as 7.60 ± 0.08 for NHA-AT_{1A} and 7.67 ± 0.07 for NHA-AT_{1A}-EGFP. PD123319, an AT_2 receptor selective nonpeptide antagonist, did not significantly displace the labeled peptide as indicated by pK_I values <6.0 for both receptors.

The signaling capacity of the NHA-AT_{1A}-EGFP receptor

was compared with the wild-type (NHA-AT_{1A}) receptor using a Cytosensor Microphysiometer, which measures the rate of change of pH as an index of overall cell activation. Concentration-response curves were constructed over the concentration range 10^{-11} to 10^{-6} M (Fig. 1B) and corresponding pEC_{50} values were determined. For the NHA-AT_{1A}-EGFP receptor, a pEC_{50} value of 8.34 ± 0.10 was observed that was not significantly different from that of the wild-type NHA-AT_{1A} (8.10 ± 0.16). The maximum response to AngII was similar for both receptors.

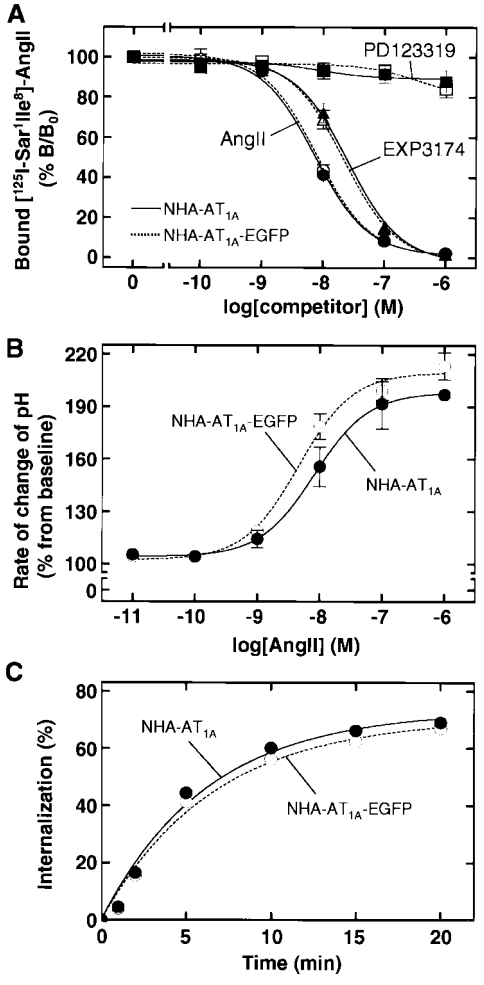

Fig. 1. Comparison of ligand affinity, signaling capacity, and internalization of the NHA-AT_{1A} and NHA-AT_{1A}-EGFP receptors transiently expressed in CHO-K1 cells. A, competition binding assay for [^{125}I]Sar^{1}Ile^{8}AngII displaced with AngII, EXP3174, and PD123319 for the NHA-AT_{1A} (filled symbols, solid lines) or NHA-AT_{1A}-EGFP (empty symbols, dashed lines) receptors. Binding assays (5 h, 4°C) were performed with ~30 pmol of [^{125}I]Sar^{1}Ile^{8}AngII (60,000 cpm) in the presence of increasing concentrations of competing ligand. Data are mean ± S.E. from four experiments. B, signaling of the NHA-AT_{1A} (–●–) and NHA-AT_{1A}-EGFP (- -○- -) receptors was measured by a Cytosensor Microphysiometer. Cells transiently expressing the NHA-AT_{1A} or NHA-AT_{1A}-EGFP receptors was perfused with various concentrations of AngII and the rate of pH change of the surrounding fluid was measured. Data are expressed as the percentage change from baseline (normalized to 100%) and represented as mean ± S.E. from three experiments. C, radioligand internalization comparing the NHA-AT_{1A} (–●–) and NHA-AT_{1A}-EGFP (- -○- -) receptors. Cells transiently expressing the NHA-AT_{1A} or NHA-AT_{1A}-EGFP receptors were incubated with [^{125}I]AngII at 37°C for indicated times. Bound ligand was stripped from the cell surface receptors and the amount of intracellular radioactivity was expressed as a percentage of the total specifically bound counts (intracellular + cell surface). Data are mean ± S.E. of four experiments.

Fig. 1C shows a comparison of the time course of internalization for the NHA-AT_{1A} and NHA-AT_{1A}-EGFP receptors, measured by the radio-ligand [^{125}I]AngII method. The two receptors internalized rapidly and with similar kinetics, reaching a maximum (NHA-AT_{1A}: 73.5 ± 2.3%, NHA-AT_{1A}-EGFP: 70.8 ± 2.4%) with $t_{1/2}$ of 4.3 ± 0.2 min for the wild-type and 4.6 ± 0.2 min for the EGFP-tagged receptor (n = 4). These results indicate that the addition of EGFP to the carboxyl terminus of the AT_{1A} receptor does not influence the rate or degree of receptor endocytosis.

AngII also induced a similar magnitude and kinetics of receptor phosphorylation: a rapid 3-fold increase from basal was observed for both wild-type and EGFP-tagged receptors, peaking at 5 min, after which a steady level was maintained (data not shown).

Internalization of NHA-AT_{1A}-EGFP Receptor Measured by Confocal Microscopy. AngII-induced internalization of the NHA-AT_{1A}-EGFP receptor was examined by confocal microscopy in CHO-K1 cells that transiently expressed the receptor (see Fig. 2). Cells expressing a moderate level of receptor were chosen and optical sections were taken through cells at a point where the nucleus was largest. To differentiate between cell surface receptor and intracellular receptor, the plasma membrane of cells was defined by staining with a WGA-TR conjugate, which binds to carbohydrates on the cell surface of nonpermeabilized cells.

For each cell, images of the green fluorescence (AT_{1A}-EGFP) and the red fluorescence (WGA-TR) were collected separately. In a computer overlay of the two images (Fig. 2A), yellow is generated where the two colors colocalize. By calculating the percentage of green fluorescence that is not coverted to yellow relative to the total green fluorescence signal, we were able to quantify intracellular (and thereby internalized) receptor.

Before stimulation, the majority of EGFP fluorescence was spread evenly across the cell surface, with some spots in perinuclear structures and diffuse staining throughout the cytosol. Thirty to forty percent of EGFP fluorescence was cytoplasmic in untreated cells (Fig. 2, B and C, 0 min). After AngII stimulation (10^{-7} M), fluorescence appeared in large spots in the cytoplasm—presumably endocytic vesicles (Fig. 2B). At 1 min, receptor aggregated on the membrane and spots appeared adjacent to the membrane. At 2 min, green fluorescent spots were deeper in the cytoplasm. At 5, 10, and 20 min, the fluorescent spots remained cytoplasmic. The proportion of green fluorescence in the cytoplasm was quantified after the initial rapid translocation of receptor from the cell surface ($t_{1/2}$, 2.1 ± 0.9, n = 3); receptor internalization reached a maximum of 70 to 75% at 5 min, then reached a plateau. For subsequent experiments, stimulation with AngII and analogs was for 20 min.

The effect of various concentrations of AngII on internalization is shown in Fig. 3A. Cells were stimulated with AngII for 20 min at concentrations ranging from 10^{-11} to 10^{-7} M. The pEC_{50} for this response was calculated as 9.27 ± 0.27, which is comparable with the affinity of AngII at the AT_{1A} receptor (Chiu et al., 1993). Maximum internalization (~75%) was observed at 10^{-7} M, corresponding to a concentration 100 times the K_D of AngII at the AT_{1A} receptor. This concentration of AngII was used to determine specificity.

Internalization of the NHA-AT_{1A}-EGFP receptor was the result of a specific interaction between AngII and the recep-

tor (Fig. 3B). The selective AT_1 nonpeptide antagonist, EXP3174 (10^{-5} M), which binds with high affinity to residues within the transmembrane domains of the receptor, at a distinct, yet overlapping site to that of AngII (Hunyady et al., 1996), alone did not cause internalization. However, pretreatment with the antagonist for 20 min (10^{-5} M) completely prevented the internalization induced by AngII stimulation (10^{-7} M, $n = 3$).

Internalization by Substituted Analogs of AngII. Cells expressing the NHA-AT_{1A}-EGFP receptor were stimulated for 20 min with analogs of AngII at a concentration equal to 100-fold the K_D of that analog at the AT_{1A} receptor (Table 1). Saturating concentrations and the 20-min time-point were chosen to allow maximal internalization of each analog. Because substitutions in AngII at positions 4 and 8 lead to profound decreases in AT_{1A} receptor activation, as measured by inositol phosphate generation [see Table 1 (Miura et al., 1999; Miura and Karnik, 1999)], we measured the internalization caused by AngII with analogs substituted

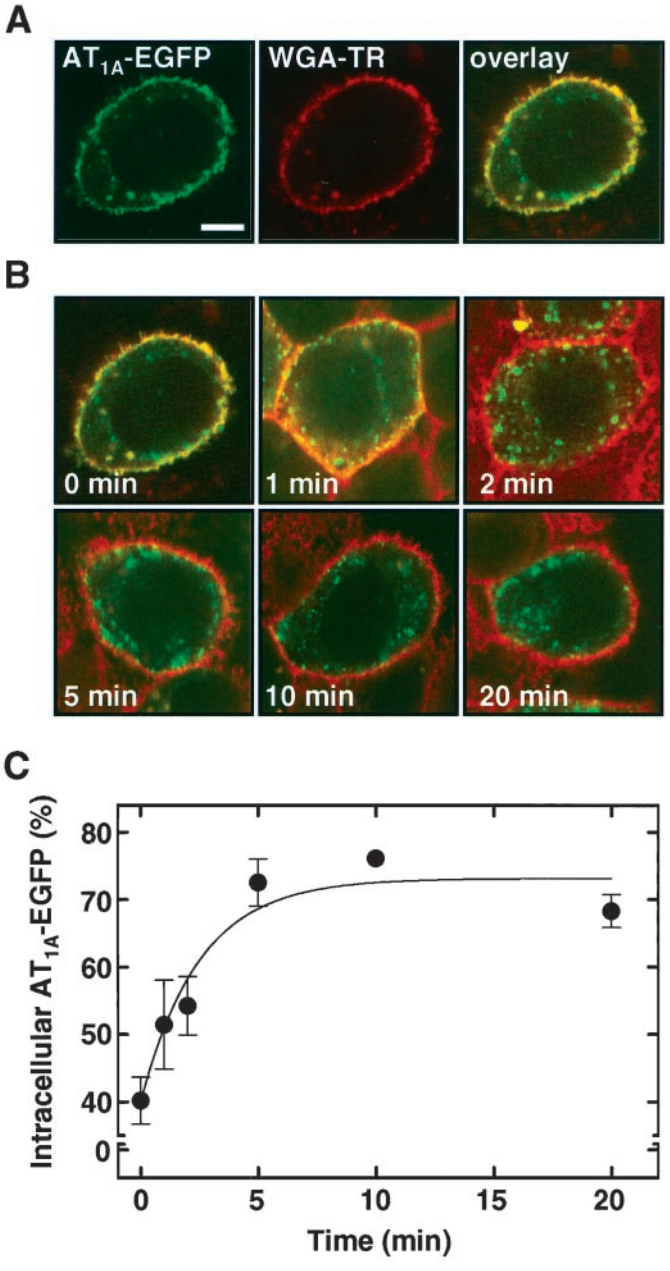

Fig. 2. Confocal imaging and time-dependence of internalization of the NHA-AT_{1A}-EGFP receptor transiently expressed in CHO-K1 cells. A, single optical section of a transfected CHO-K1 cell taken with a confocal microscope. Left, NHA-AT_{1A}-EGFP receptor fluorescence (green, labeled AT_{1A}-EGFP) for an unstimulated cell. Scale bar, 2 μm. Middle, wheat-germ agglutinin-Texas Red (red, labeled WGA-TR) fluorescence bound to the cell membrane of the same cell. Right, an overlay of red and green images resulting in a yellow pseudocolor, where red and green colocalize. B, CHO-K1 cells expressing the AT_{1A}-EGFP receptor were stimulated with AngII (10^{-7} M) for 0, 1, 2, 5, 10 and 20 min, fixed, and stained with WGA-TR. Representative overlay pictures are shown for each time-point. C, the proportion of intracellular receptor was quantified for nine cells at each time-point (as described under *Materials and Methods*). Data are mean ± S.E. of three experiments.

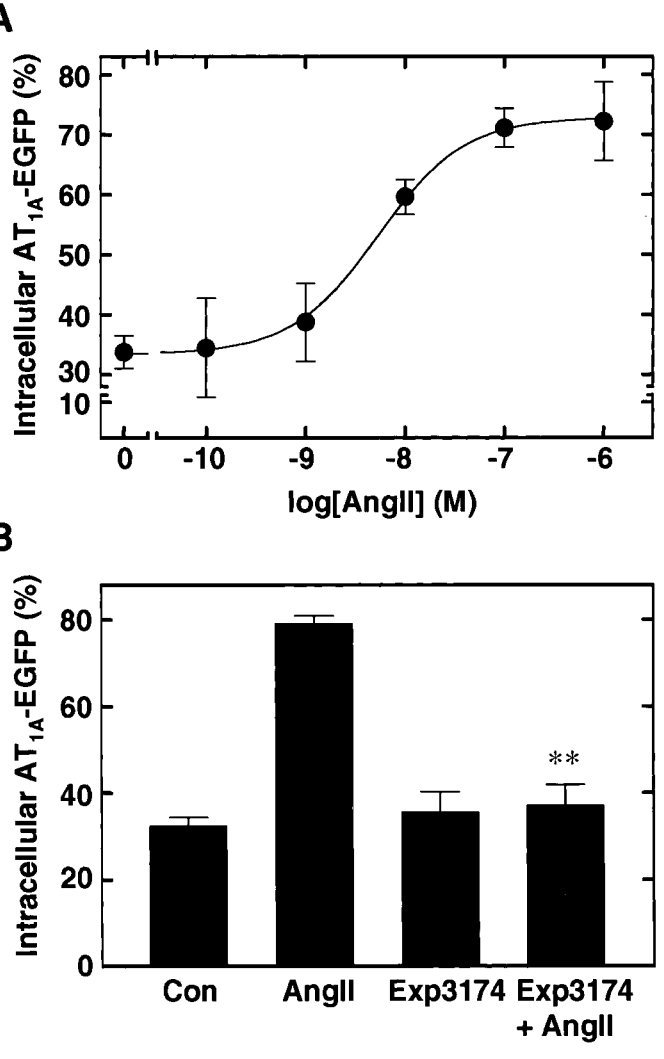

Fig. 3. Characterization of AT_{1A}-EGFP receptor internalization. A, concentration-response curve for NHA-AT_{1A}-EGFP receptor internalization. Cells expressing the receptor were stimulated with AngII at concentrations over the range 10^{-11} to 10^{-7} M for 20 min. The proportion of intracellular receptor was measured by confocal microscopy and the concentration response-curve exhibited a pEC_{50} of 9.27 ± 0.27. Data are mean ± S.E. of three experiments, nine cells per concentration in each experiment. B, the nonpeptide AT_1 receptor antagonist EXP3174 does not stimulate internalization of the NHA-AT_{1A}-EGFP receptor and inhibits AngII-mediated internalization. Cells expressing the NHA-AT_{1A}-EGFP receptor were stimulated with AngII (10^{-7}M, 20 min), EXP3174 (10^{-5}M, 20 min) or with AngII (10^{-7}M, 20 min) after pretreatment with EXP3174 (10^{-5}M, 20 min), and processed for confocal microscopy. (**, $p < 0.01$ of AngII; Con, unstimulated).

at these positions. As shown in Fig. 4A, both mono-substituted (Sar^1Ala^4AngII, Sar^1Ala^8AngII) and di-substituted analogs ($Sar^1Ile^4Ile^8AngII$, $Sar^1Gly^4Gly^8AngII$) induced full internalization of the NHA-AT_{1A}-EGFP receptor.

Internalization of the NHA-AT_{1A}-EGFP receptor caused by AngII analogs substituted at other positions was also examined (Table 1, Fig. 4B). AngIII is an aminopeptidase product of AngII (des-Asp^1AngII), and an endogenous agonist at the AT_1 receptor (Freeman et al., 1977; de Gasparo et al., 2000). Like AngII, it caused full internalization of the NHA-AT_{1A}-EGFP receptor (Fig. 4B). Substitutions of Arg^2 to glutamine, and the α-carboxyl of Phe^8 to amide, which significantly reduce binding affinity (Table 1), were found to have a negligible effect on the amount of internalization compared with AngII. In addition, changing Asp^1 to alanine, Val^3 to alanine, His^6 to alanine, or Pro^7 to alanine, residues important for peptide conformation and stability (Regoli et al., 1974), had no observable effect on internalization.

AT_{1A} Receptor Phosphorylation by AngII Analogs. We examined the capacity of the various AngII analogs to cause phosphorylation of the AT_{1A} receptor, expressed in CHO-K1 cells, using the N-terminal HA tag to immunoprecipitate the receptor. AngII caused a robust phosphorylation of the AT_{1A} receptor (Fig. 5). Maximal receptor phosphorylation in response to AngII is observed at concentrations 10- to 100-fold higher than the K_D and at 10 min after ligand stimulation (Thomas et al., 2000). In comparison to AngII, substitutions at Arg^2 (G2), Val^3 (A3), Tyr^4 (A4), His^6 (A6), and Pro^7 (A7) or substitution of the α-carboxyl group of Phe^8 (Am) had no significant effect on receptor phosphorylation. In contrast, alanine substitution of Asp^1 (A1) led to a ~40% reduction in AT_{1A} receptor phosphorylation, which was mirrored by a similar reduction with AngIII (data not shown). The most important residue for phosphorylation seems to be Phe^8. Most substitutions at this position caused significant decreases in receptor phosphorylation. Single substitutions of Phe^8 to alanine (A8), β-cyclohexylalanine (a nonaromatic, saturated ring side chain of equivalent size and hydrophobicity to phenylalanine/tyrosine) (C8), isoleucine (I8), or diphenylalanine (a strongly aromatic side chain of increased size compared with phenylalanine/tyrosine) (D8) caused significant (45 to 70%) decreases in AT_{1A} receptor phosphorylation compared with AngII. Double isoleucine substitution at

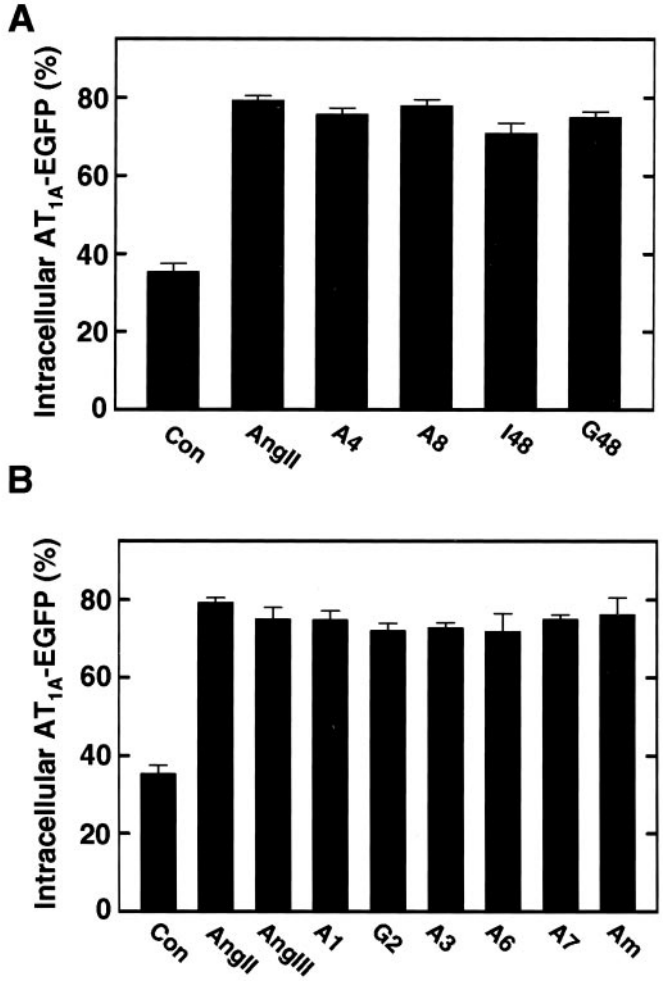

Fig. 4. Effect of substitution of AngII side chains on AT_{1A}-EGFP receptor internalization. A, internalization of NHA-AT_{1A}-EGFP receptor by analogs of AngII substituted at positions 4 and 8. Cells expressing the NHA-AT_{1A}-EGFP receptor were stimulated for 20 min at a concentration of 100 $\times$ K_D of the specified analog and intracellular receptor quantified by confocal microscopy. (A4, Sar^1Ala^4AngII; A8, Sar^1Ala^8AngII; I48, $Sar^1Ile^4Ile^8AngII$; G48, $Sar^1Gly^4Gly^8AngII$; Con: unstimulated). B, NHA-AT_{1A}-EGFP receptor internalization by analogs of AngII substituted at positions 1, 2, 3, 6, 7, and the α-carboxyl group of Phe^8 (see Table 1). Cells expressing the receptor were stimulated for 20 min at a concentration of 100 $\times$ K_D of specified analogs. (A1, Ala^1AngII. G2, Sar^1Gln^2AngII; A3, Sar^1Ala^3AngII; A6, Sar^1Ala^6AngII; A7, Sar^1Ala^7AngII; Am, Sar^1AngII-$CONH_2$). Quantification was performed by confocal microscopy from nine cells/analog/experiment. Data are mean ± S.E. of four experiments. AngII analog codes are from Table 1.

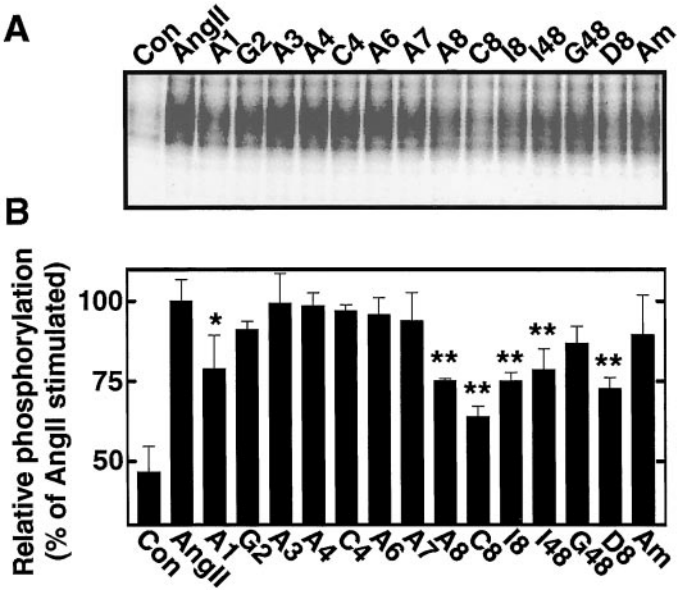

Fig. 5. Phosphorylation of the NHA-AT_{1A} receptor transiently expressed in CHO-K1 cells stimulated with AngII analogs. A, CHO-K1 cells expressing the receptor were preloaded with 0.2 mCi/ml [^{32}P]P_i and stimulated for 20 min with AngII or substituted analogs of AngII at concentrations 100 times their respective K_D (see Table 1). The cells were lysed and the receptor immunoprecipitated and resolved on a 10% SDS-PAGE gel. Radioactively labeled receptors were visualized and quantified with a filmless autoradiographic system (Fujix Bio-imaging Analyzer BAS 1000) and presented as a percentage of the phosphorylation caused by AngII. The phosphorylated receptor migrates as a broad band running at 60 to 110 kDa. B, gels were quantified according to the band intensity and expressed as a percentage of the phosphorylation induced by AngII (100%). Data are mean ± S.E. of three experiments (*, $p < 0.05$; **, $p < 0.01$ compared with AngII). AngII analog codes are from Table 1; Con, unstimulated.

positions 4 and 8 (I48) decreased receptor phosphorylation similar to the single isoleucine substitution at position 8 (I8), consistent with a lack of effect of position 4 substituted analogs on receptor phosphorylation. Remarkably, the double substitution to glycine at position 4 and 8 (G48) did not significantly reduce receptor phosphorylation compared with AngII. So, although single substitutions at Phe^8 can inhibit receptor phosphorylation somewhat, there was no clear preference for size, hydrophobicity, or aromaticity at this position. Moreover, based on the strong phosphorylation induced by G48, it would seem that the presence of both "agonism" defining residues, Tyr^4 and Phe^8, is not essential for AT_{1A} receptor phosphorylation.

Activation of MAP Kinase by AngII Analogs. Previous studies on the structure-activity profiles of AngII analogs with respect to their ability to activate AT_1 receptor signaling have focused principally on the $G_{\alpha q/11}$-PLC/IP_3 pathway. These studies have revealed strict requirements for position 4 and 8 in generating the active signaling form of the receptor (Miura et al., 1999; Miura and Karnik, 1999). To examine whether other signaling pathways activated by the AT_{1A} receptor are similarly affected by substitutions in AngII, the activation of MAPK (p42/44; extracellular signal-regulated kinase) after stimulation by the series of AngII analogs was determined (Fig. 6). AngII stimulation (4 min at 37°C) of the AT_{1A} receptor lead to a robust (~6-fold) increase in MAPK activation, primarily through activation of p42. Substitutions at position 1, 2, 3, 4, 6, and 7, the α-carboxyl of Phe^8, and the substitution of Phe^8 with diphenylalanine produced levels of MAPK activation similar to that of AngII. In contrast, substitution of Phe^8 with alanine completely abolished activation. Single substitutions of Phe^8 with β-cyclohexylalanine or isoleucine also significantly reduced MAPK activation compared with AngII. Similarly, double isoleucine and glycine substitutions of Tyr^4 and Phe^8 peptides weakly activated MAPK.

Discussion

A major initial aim of this study was to generate an AT_{1A}-EGFP chimeric receptor, which would allow visualization and quantification of AT_{1A} receptor endocytosis using confocal microscopy. Direct quantification was preferred because previous methods for examining AT_1 receptor internalization have been predominantly indirect (e.g., acid-insensitive sequestration of radioactive AngII). The unobtrusive nature of the carboxyl-terminal EGFP tag on AT_{1A} receptor binding affinity, selectivity, and receptor-mediated cellular activation was confirmed by competition binding experiments, Cytosensor measurements, and receptor phosphorylation assays. That these parameters were indistinguishable for EGFP-tagged and -untagged AT_{1A} receptors agrees with studies on other GFP-tagged GPCRs (Milligan, 1999) and with a recent report (Miserey-Lenkei et al., 2001), in which an AT_{1A}-EGFP receptor was used to investigate AT_{1A} receptor trafficking in human embryonic kidney 293 cells.

AT_{1A}-EGFP receptor internalization was quantified using confocal microscopy, using staining with WGA-TR to delineate the cell surface. Receptor endocytosis measured in this way was qualitatively equivalent to the traditional acid-insensitive [^{125}I]AngII binding method: internalization was rapid ($t_{1/2}$ = 2.1 min) and reached a steady state by 10 to 20 min, indicating that ligand sequestration correlates with receptor internalization. The pEC_{50} of AT_{1A}-EGFP receptor internalization as determined by confocal microscopy (9.27 ± 0.27) approximated the K_D value of AngII at the AT_{1A} receptor (~ 1 nM), which highlights the close relationship between ligand binding and internalization. The graded response to AngII demonstrates that the assay can distinguish different levels of receptor internalization. The nonpeptide antagonist EXP3174 caused no internalization of the AT_{1A}-EGFP receptor, demonstrating that ligand binding to the receptor is not sufficient for internalization and that additional points of contact, or conformational changes in the receptor not provided by EXP3174, are required for this process. Importantly, the internalization in response to AngII was prevented by EXP3174, verifying that a specific interaction between AngII and the AT_{1A} receptor causes internalization.

The principal, yet unexpected, finding of our study was that AT_{1A} receptor internalization is unaffected by substitutions at any position within the AngII peptide sequence. This result contrasts with the accepted view that the two aromatic amino acid side-chains of AngII, Tyr^4 and Phe^8, are required for activating IP_3 signaling through the AT_1 receptor. Sub-

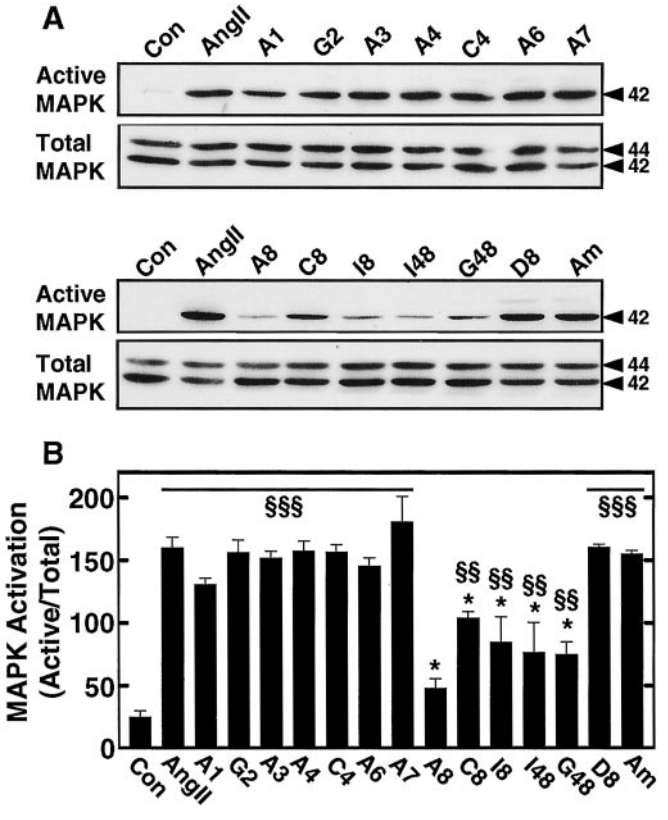

Fig. 6. MAPK activation induced by AngII analogs. A, cells expressing the AT_{1A} receptor were stimulated for 4 min (maximum activation) with AngII or substituted analogs of AngII at concentrations 100 times their respective K_D. Cells were lysed and cellular proteins resolved on 10% SDS-PAGE followed by Western blotting. Blots were probed with a monoclonal antibody (E10) to phospho-p44/42 MAPK (T202/Y204) to identify the phosphorylated (active) forms of MAPK and reprobed with a rabbit polyclonal antibody (SC93) to detect total MAPK. Blots were developed using enhanced chemiluminescence and band intensity quantified (B) using Scion Image software. Active MAPK was normalized for loading differences using the intensity of the corresponding Total MAPK lane. The data are means ± S.E. from three to five experiments. ***, $p < 0.001$ compared with AngII; §§, $p < 0.01$ compared with control; §§§, $p < 0.001$ compared with control. AngII analog codes are from Table 1.

stitution of these residues, reducing their bulk and removing their aromaticity, has been shown in vivo, in isolated tissues, (Regoli et al., 1974; Samanen et al., 1989), and in cells expressing a recombinant AT_1 receptor (Noda et al., 1996; Miura et al., 1999), to significantly reduce responses compared with AngII. Substitution of Phe^8 or Tyr^4 with isoleucine yields peptides with reduced ability to generate IP_3 (~20% and 80% of AngII, respectively) (Miura et al., 1999), yet we observed no effect of these two individual substitutions on the level of internalization. Even the di-substituted analogs ($Sar^1Ile^4Ile^8$AngII and $Sar^1Gly^4Gly^8$AngII) that display no agonism with respect to inositol phosphate signaling (see Table 1) gave full AT_{1A}-EGFP receptor internalization. Consistent with our findings, previous studies have reported strong sequestration of [^{125}I]Sar^1Ile^8AngII (Conchon et al., 1994; Thomas et al., 1996) and other Phe^8 analogs of AngII also cause AT_{1A}-EGFP receptor internalization (Misersey-Lenkei et al., 2001). This evidence shows that the AngII residues involved in coupling the receptor to inositol phosphate signaling are not required for receptor internalization, indicating that distinct ligand-receptor interactions and receptor conformations subserve PLC signaling and internalization.

Given that phosphorylation within the central region of the AT_{1A} carboxyl terminus is associated with receptor internalization (Smith et al., 1998; Thomas et al., 1998), we investigated whether substitutions in AngII would affect receptor phosphorylation. Only changes to Asp^1 (to alanine) and Phe^8 were found to inhibit phosphorylation significantly, although none completely. A comparison of Phe^8-substituted AngII analogs revealed similar reduced phosphorylation for alanine, isoleucine, diphenylalanine, and β-cyclohexylalanine replacement, suggesting that neither position 8 side chain size, hydrophobicity, nor aromaticity is predominant in determining AT_{1A} receptor phosphorylation. Moreover, double substitution on Tyr^4 and Phe^8 with isoleucine produced a level of phosphorylation similar to the single isoleucine replacement for Phe^8, indicating a minimal contribution of Tyr^4 to AT_{1A} phosphorylation. This result was surprising because mutation of Asn^{111} in the AT_{1A} receptor, the residue presumed to make productive contact with Tyr^4 of AngII, produces a receptor incapable of AngII-induced phosphorylation (Thomas et al., 2000). Remarkably, double-glycine substitution of Tyr^4 and Phe^8 produced a level of receptor phosphorylation equivalent to that generated by AngII, which would seem difficult to reconcile given the contribution of position 8 revealed by the other analogs. We can only speculate that removal of the Phe^8 (and Tyr^4) side chains favors a phosphorylatable conformation.

An additional insight into the differing requirements for receptor function is provided by the activation of MAPK by the AngII analogs. Alanine was the least tolerated residue at position 8, resulting in little MAPK activation. In contrast, β-cyclohexylalanine (nonaromatic) or isoleucine (nonpolar) substitution was moderately tolerated, whereas diphenylalanine (strongly aromatic) was fully tolerated, indicating a key contribution of side chain aromaticity and perhaps hydrophobicity to MAPK activation. Single substitutions of Tyr^4 to alanine (A4) and β-cyclohexylalanine (C4) failed to reduce MAPK activation compared with AngII and $Sar^1Ile^4Ile^8$AngII (I48) produced a similar level of MAPK activation to Sar^1Ile^8AngII (I8). Thus, in contrast to inositol phosphate signaling, where substitution with β-cyclohexylalanine at Tyr^4 (C4) leads to significant inhibition of signaling, Tyr^4 seems to contribute little to MAPK signaling. Moreover, double substitution at Tyr^4 and Phe^8, with isoleucine or glycine, which abrogates inositol phosphate signaling, reduces MAPK signaling by only half.

Shown in Fig. 7 are separate comparisons of receptor internalization, inositol phosphate production, phosphorylation and MAPK activation, with respect to each other, after stimulation by AngII and the substituted analogs. These comparisons reveal differences in the tolerance of the various receptor processes to substitutions in AngII. For example, when internalization is compared separately with inositol phosphate production (Fig. 7A), phosphorylation (Fig. 7B), and MAPK activation (Fig. 7C), it is clear that the di-substituted analogs ($Sar^1Ile^4Ile^8$AngII and $Sar^1Gly^4Gly^8$AngII; I48 and G48) promote full receptor internalization, slightly reduced (80 to 90% of AngII) phosphorylation (Fig. 7B), a re-

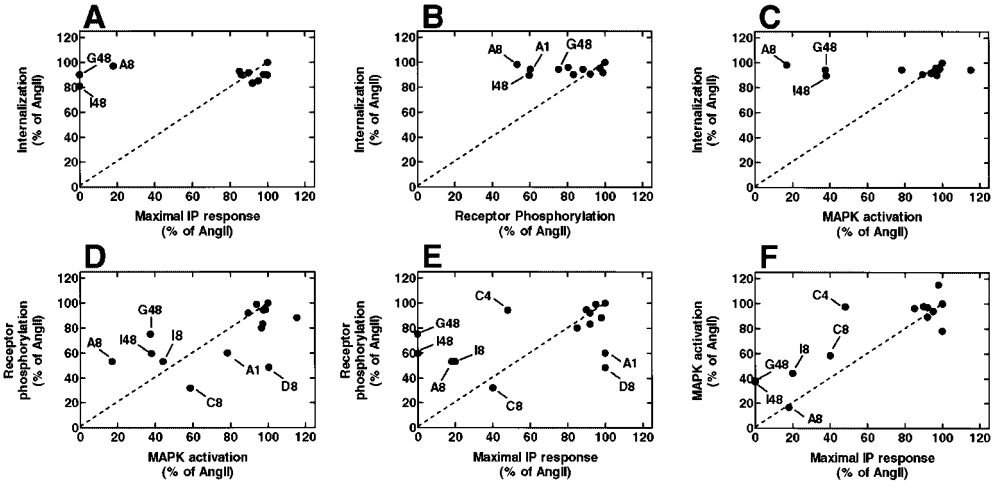

Fig. 7. Comparison of individual receptor activities in response to stimulation by AngII analogs. Data for receptor internalization (Fig. 4), phosphorylation (Fig. 5), MAPK activation (Fig. 6), and inositol phosphate production (Table 1) were expressed as a percentage of AngII (100%). Values are corrected for basal values of the unstimulated control samples. This normalized data for the individual receptor processes was plotted to compare all receptor activities. A theoretical line (dashed), representing the position at which a particular substitution would affect two receptor functions to the same degree, is shown. For clarity, only analogs whose responses are shifted from full activity are labeled using the code described in Table 1.

duced (40% of AngII) MAPK activation (Fig. 7C), and completely fail to elicit inositol phosphate production (Fig. 7A). Ala[1]AngII (A1) fully activates IP and MAPK, but shows a slight reduction (60% of AngII) in receptor phosphorylation (Fig. 7B). Sar[1]Ala[8]AngII (A8) elicits greatly reduced IP and MAPK responses (20% of AngII) and reduced capacity for phosphorylation (50% of AngII, Fig. 7B). Figure 7D highlights the structural requirements for position 8 with respect to receptor phosphorylation and MAPK activation. Although substitution Phe[8] with isoleucine (I8) reduced phosphorylation (50% of AngII) and MAPK activation (40% of AngII), substitution with the strongly aromatic diphenylalanine (D8) causes reduced (50%) receptor phosphorylation but full MAPK activation. An AngII peptide carrying the nonaromatic ring side chain, β-cyclohexylalanine, at position 8 (C8) reduces receptor phosphorylation (30% of AngII) more than reducing MAPK activation (60% of AngII). These results suggest that aromaticity and bulk at position 8, although important for MAPK activation, are not crucial for phosphorylation. The bulky, but not aromatic, substitution at position 4 (Sar[1]Cha[4]AngII, C4) produces a ligand that promotes full phosphorylation (Fig. 7E) and MAPK (Fig. 7F) but only an intermediate inositol phosphate response. These data demonstrate differing structural and size requirements in the AngII peptide for AT_{1A} receptor activation, signaling, phosphorylation and internalization.

Multiple functional ligand-receptor contacts, variously referred to as agonist-receptor trafficking (Kenakin, 1995) or biased agonism (Jarpe et al., 1998), support the concept of separate receptor conformational states. Based on contemporary two- or three-state models for GPCR activation (Lefkowitz et al., 1993; Kenakin, 1995; Leff, 1995; Leff et al., 1997; Leurs et al., 1998; Scaramellini and Leff, 1998), receptor conformations that activate signaling (e.g., R*) are also targeted for phosphorylation by GPCR kinases, leading to arrestin binding, which inhibits further signaling and targets receptors for clathrin-mediated internalization. Thus, substitutions in the AngII peptide (specifically at Tyr[4] and Phe[8]) should equally affect signals emanating from the receptor, phosphorylation and internalization. Instead, we observed differences in the capacity of AngII analogs to promote receptor signaling, phosphorylation, and internalization. Most compelling was the observation that all substituted analogs stimulated robust AT_{1A} receptor internalization, indicating that internalization is more tolerant than signaling of modifications in the AngII peptide. These data argue strongly against a linear transition from an inactive to a signaling receptor, which is then phosphorylated, desensitized, and internalized. Instead, they support the idea of ligand-specific receptor states, each selected by unique contacts between peptide and receptor and potentially capable of coupling to one or more distinct receptor activities. A caveat to this interpretation is that we used saturating concentrations of ligand with single, maximal time-points of stimulation in one cell type (CHO-K1). Clearly, cellular environment (i.e., the complement and/or concentration of G proteins and other signaling and regulatory molecules) may affect the capacity of specific analogs to promote signaling, phosphorylation, and internalization. Also, experiments measuring initial rates of reactions may reveal subtle differences in the kinetics and/or efficacy of substituted AngII analogs not revealed by the current experimental approach.

Nevertheless, the concept of distinct AT_{1A} receptor states is consistent with AT_{1A} receptor mutants that display proclivity for specific receptor functions. For example, an Asp[74]Asn AT_{1A} mutant undergoes full internalization yet does not signal (Conchon et al., 1994; Miserey-Lenkei et al., 2001); an AT_{1A} receptor carrying five tyrosine mutations is deficient in inositol phosphate and calcium signaling (Doan et al., 2001) but retains robust AngII-induced intracellular tyrosine kinase signaling and cell proliferation; and AngII causes internalization, but not phosphorylation, of constitutively active AT_{1A} receptor mutants (Thomas et al., 2000).

Acknowledgments

We thank John Feutrill for cloning the NHA-AT_{1A}-EGFP receptor construct.

References

Chiu AT, Dunscomb J, Kosierowski J, Burton CR, Santomenna LD, Corjay MH, and Benfield P (1993) The ligand binding signatures of the rat AT1A, AT1B and the human AT1 receptors are essentially identical. *Biochem Biophys Res Commun* **197:**440–449.

Conchon S, Monnot C, Teutsch B, Corvol P, and Clauser E (1994) Internalization of the rat AT1a and AT1b receptors: pharmacological and functional requirements. *FEBS Lett* **349:**365–370.

de Gasparo M, Catt KJ, Inagami T, Wright JW, and Unger T (2000) International union of pharmacology. XXIII. The angiotensin II receptors. *Pharmacol Rev* **52:** 415–472.

Doan TN, Ali MS, and Bernstein KE (2001) Tyrosine kinase activation by the angiotensin II receptor in the absence of calcium signaling. *J Biol Chem* **276:** 20954–20958.

Feng YH, Noda K, Saad Y, Liu XP, Husain A, and Karnik SS (1995) The docking of Arg2 of angiotensin II with Asp281 of AT1 receptor is essential for full agonism. *J Biol Chem* **270:**12846–12850.

Freeman RH, Davis JO, Lohmeier TE, and Spielman WS (1977) [Des-Asp1] angiotensin II: mediator of the renin-angiotensin system? *Fed Proc* **36:**1766–1770.

Hunyady L, Balla T, and Catt KJ (1996) The ligand binding site of the angiotensin AT1 receptor. *Trends Pharmacol Sci* **17:**135–140.

Hunyady L, Catt KJ, Clark AJ, and Gaborik Z (2000) Mechanisms and functions of AT_1 angiotensin receptor internalization. *Regul Pept* **91:**29–44.

Jarpe MB, Knall C, Mitchell FM, Buhl AM, Duzic E, and Johnson GL (1998) [D-Arg1, D-Phe5, D-Trp7,9, Leu11]Substance P acts as a biased agonist toward neuropeptide and chemokine receptors. *J Biol Chem* **273:**3097–3104.

Kenakin T (1995) Agonist-receptor efficacy. II. Agonist trafficking of receptor signals. *Trends Pharmacol Sci* **16:**232–238.

Leff P (1995) The two-state model of receptor activation. *Trends Pharmacol Sci* **16:**89–97.

Leff P, Scaramellini C, Law C, and McKechnie K (1997) A three-state receptor model of agonist action. *Trends Pharmacol Sci* **18:**355–362.

Lefkowitz RJ (1998) G protein-coupled receptors. III. New roles for receptor kinases and beta-arrestins in receptor signaling and desensitization. *J Biol Chem* **273:** 18677–18680.

Lefkowitz RJ, Cotecchia S, Samama P, and Costa T (1993) Constitutive activity of receptors coupled to guanine nucleotide regulatory proteins. *Trends Pharmacol Sci* **14:**303–307.

Leurs R, Smit MJ, Alewijnse AE, and Timmerman H (1998) Agonist-independent regulation of constitutively active G-protein- coupled receptors. *Trends Biochem Sci* **23:**418–422.

Milligan G (1999) Exploring the dynamics of regulation of G protein-coupled receptors using green fluorescent protein. *Br J Pharmacol* **128:**501–510.

Miserey-Lenkei S, Lenkei Z, Parnot C, Corvol P, and Clauser E (2001) A functional enhanced green fluorescent protein (EGFP)-tagged angiotensin II AT_{1A} receptor recruits the endogenous Galphaq/11 protein to the membrane and induces its specific internalization independently of receptor-G protein coupling in HEK-293 cells. *Mol Endocrinol* **15:**294–307.

Miura S, Feng YH, Husain A, and Karnik SS (1999) Role of aromaticity of agonist switches of angiotensin II in the activation of the AT1 receptor. *J Biol Chem* **274:**7103–7110.

Miura S and Karnik SS (1999) Angiotensin II type 1 and type 2 receptors bind angiotensin II through different types of epitope recognition. *J Hypertens* **17:**397–404.

Noda K, Feng YH, Liu XP, Saad Y, Husain A, and Karnik SS (1996) The active state of the AT1 angiotensin receptor is generated by angiotensin II induction. *Biochemistry* **35:**16435–16442.

Noda K, Saad Y, and Karnik SS (1995) Interaction of Phe8 of angiotensin II with Lys199 and His256 of AT1 receptor in agonist activation. *J Biol Chem* **270:**28511–28514.

Oakley RH, Laporte SA, Holt JA, Barak LS, and Caron MG (2001) Molecular determinants underlying the formation of stable intracellular G protein-coupled receptor-beta -arrestin complexes after receptor endocytosis*. *J Biol Chem* **276:** 19452–19460.

Pierce KL, Luttrell LM, and Lefkowitz RJ (2001) New mechanisms in heptahelical receptor signaling to mitogen activated protein kinase cascades. *Oncogene* **20:** 1532–1539.

Regoli D, Park WK, and Rioux F (1974) Pharmacology of angiotensin. *Pharmacol Rev* **26:**69–123.
Samanen J, Cash T, Narindray D, Brandeis E, Yellin T, and Regoli D (1989) The role of position 4 in angiotensin II antagonism: a structure-activity study. *J Med Chem* **32:**1366–1370.
Scaramellini C and Leff P (1998) A three-state receptor model: predictions of multiple agonist pharmacology for the same receptor type. *Ann NY Acad Sci* **861:**97–103.
Smith RD, Hunyady L, Olivares-Reyes JA, Mihalik B, Jayadev S, and Catt KJ (1998) Agonist-induced phosphorylation of the angiotensin AT1a receptor is localized to a serine/threonine-rich region of its cytoplasmic tail. *Mol Pharmacol* **54:**935–941.
Southwell BR, Seybold VS, Woodman HL, Jenkinson KM, and Furness JB (1998) Quantitation of neurokinin 1 receptor internalization and recycling in guinea-pig myenteric neurons. *Neuroscience* **87:**925–931.
Thomas WG (1999) Regulation of angiotensin II type 1 (AT1) receptor function. *Regul Pept* **79:**9–23.
Thomas WG, Motel TJ, Kule CE, Karoor V, and Baker KM (1998) Phosphorylation of the angiotensin II (AT1A) receptor carboxyl terminus: a role in receptor endocytosis. *Mol Endocrinol* **12:**1513–1524.
Thomas WG, Qian H, Chang CS, and Karnik S (2000) Agonist-induced phosphorylation of the angiotensin II (AT_{1A}) receptor requires generation of a conformation that is distinct from the inositol phosphate-signaling state. *J Biol Chem* **275:**2893–2900.
Thomas WG, Thekkumkara TJ, and Baker KM (1996) Cardiac effects of AII. AT1A receptor signaling, desensitization, and internalization. *Adv Exp Med Biol* **396:** 59–69.
Thomas WG, Thekkumkara TJ, Motel TJ, and Baker KM (1995) Stable expression of a truncated AT1A receptor in CHO-K1 cells. The carboxyl-terminal region directs agonist-induced internalization but not receptor signaling or desensitization. *J Biol Chem* **270:**207–213.

Address correspondence to: Dr. Walter G. Thomas, Molecular Endocrinology Laboratory, Baker Medical Research Institute, PO Box 6492, St. Kilda Rd. Central, Melbourne 8008, Australia. E-mail: walter.thomas@baker.edu.au